

NWRI CONTRIBUTION 87-152

Proceedings of IUTAM "Symposium on Nonlinear Water Waves",
Tokyo, Japan. Paper #31
August 25-28, 1987

**EFFECTS OF VELOCITY SHEAR ON THE
STABILITY OF SURFACE
DEEP WATER WAVE TRAINS**

by
J.C. Li¹, W.H. Hui², and M.A. Donelan³

¹ Chinese Academy of Science
Beijing, China

² University of Waterloo
Waterloo, Ontario, Canada

³ Research and Applications Branch
National Water Research Institute
Canada Centre for Inland Waters
867 Lakeshore Road, P.O. Box 5050
Burlington, Ontario, Canada L7R 4A6

September 1987

MANAGEMENT PERSPECTIVE

This paper addresses one of the complex interactions of wind and waves: the effect of the wind on the stability of small, secondary waves, referred to as side bands. The theory developed gives some insight into the controlling mechanisms, and provides insight into the growth of wave energy due to winds. Its importance is in the improvement of wave prediction models and in models of near surface velocity distributions; controlling parameters in turbulence and mixing processes in the upper layers of lakes and oceans.

Dr. J. Lawrence
Director, Research and Applications Branch
National Water Research Institute

PERSPECTIVE-GESTION

Ce rapport porte sur l'une des interactions complexes entre le vent et les vagues, à savoir l'effet du vent sur la stabilité de petites vagues secondaires appelées bandes latérales. La théorie élaborée donne un aperçu des mécanismes de commande et de l'accroissement de l'énergie des vagues sous l'action du vent. Elle tire son importance du fait qu'elle permet d'améliorer les modèles de prévision de l'état des vagues et de la distribution des vitesses près de la surface, paramètres qui influent sur les processus de turbulence et de mélange dans les couches supérieures des lacs et des océans.

Dr J. Lawrence

Directeur, Recherches et applications

Institut national de recherche sur les eaux

RÉSUMÉ

On étudie l'instabilité des bandes latérales d'un train d'ondes de Stokes en présence d'une vitesse de cisaillement uniforme. La théorie énonce en particulier que plus cette vitesse est faible, plus l'instabilité est grande et que plus elle est élevée, plus l'instabilité est faible. On a également effectué des expériences en laboratoire en présence de vagues produites mécaniquement et de vent. L'accroissement observé de l'instabilité des bandes latérales concorde du point de vue qualitatif, mais non du point de vue quantitatif, avec le modèle théorique en ce que les vents faibles - donc une faible vitesse de cisaillement - ont tendance à accroître cette instabilité et que les vents forts - donc une vitesse de cisaillement élevée - la suppriment.

EFFECTS OF VELOCITY SHEAR ON THE STABILITY OF SURFACE DEEP WATER WAVE TRAINS

J. C. Li

Chinese Academy of Science, Beijing, China

W. H. Hui

University of Waterloo, Ontario, Canada

M. A. Donelan

National Water Research Institute, Burlington, Canada

SUMMARY

The side-band instability of a Stokes wave train in uniform velocity shear is studied. In particular, theory predicts that small velocity shear tends to enhance instability whereas large velocity shear suppress it. Laboratory experiments have also been conducted on mechanically generated waves with wind blowing over them. The observed side-band growths are in qualitative, but not quantitative, agreement with the theoretical model in that gentle wind (hence smaller velocity shear generated) tends to enhance growth whereas strong wind (hence larger velocity shear) suppress it.

§1. Introduction

It is well-known that the Stokes wave train on deep water is subject to Benjamin-Feir side-band instability. Recently, however, experiments by Bliven, Huang and Long (Ref 1) at NASA Goddard Space Flight Center, and by Donelan at Canada Centre for Inland Waters (CCIW) both show that the efficiency of the Benjamin-Feir instability mechanism is reduced by wind blowing over waves. This is a very interesting and far-reaching finding, and the purpose of this paper is to propose a simple mathematical model to explain the effects of wind blowing over waves on the stability of finite amplitude wave trains.

Wind blowing over surface water waves is known to produce a phase-shifted pressure force, causing the waves to grow. At the same time it imposes a tangential force, resulting in velocity shear in the water. As a simple model to study the effects of wind on the stability of water waves, the action of the wind is represented solely by a velocity shear distributed in the water. That is to say, that we assume the action of the wind to alter the surface pressure is not important in the growth of side-band instabilities. The problem is then to investigate the effects of velocity shear on the stability of a Stokes wave train. For simplicity in the mathematical analysis, a uniform velocity shear Ω is assumed.

This model, although obviously over-simplifies the effects of wind, is shown to be capable of predicting the qualitative effects of wind on the stability of a uniform wave train.

§2. Stokes Wave Trains in Uniform Velocity Shear

2.1 Mathematical Formulation

As mentioned in the Introduction, we consider the motion of wave on water of infinite depth in the presence of uniform velocity shear; the wave motion being otherwise irrotational. Thus the velocity is of the form

$$\vec{V} = \Omega y \vec{i} + \nabla \phi(x, y, t) \quad (2.1)$$

where Ω is constant, x and y are, respectively, horizontal and upward vertical cartesian coordinates, with unit vectors \vec{i} and \vec{j} . The governing equations are

$$\nabla \cdot \vec{V} = 0 \quad (2.2)$$

$$\frac{\partial \vec{V}}{\partial t} + \vec{V} \cdot \nabla \vec{V} + \frac{\nabla p}{\rho} = -g \vec{j} \quad (2.3)$$

Substitution of Eq. (2.1) into (2.2) yields the usual Laplace equation for the potential ϕ

$$\nabla^2 \phi = 0 \quad (2.4)$$

Although the flow under study is unsteady and rotational, with velocity given by Eq. (2.1), a first integral of Eq. (2.3) still exists. Indeed, substituting (2.1) into (2.3) and integrating with respect to x and y yields the Bernoulli integral as follows

$$\frac{\partial \phi}{\partial t} + \frac{1}{2} \vec{V}^2 + \frac{p}{\rho} + gy - \frac{1}{2} \Omega^2 y^2 - \Omega \psi = \text{const.} \quad (2.5)$$

where ψ is related to ϕ by the Cauchy-Riemann conditions

$$\frac{\partial \psi}{\partial y} = \frac{\partial \phi}{\partial x}, \quad \frac{\partial \psi}{\partial x} = -\frac{\partial \phi}{\partial y} \quad (2.6)$$

The mathematical problem for calculating water wave motion of the type (2.1) is thus to solve Eq. (2.4) subject to the following boundary conditions

$$\frac{\partial \phi}{\partial y} = 0 \quad \text{at } y \rightarrow -\infty \quad (2.7)$$

$$\frac{\partial \eta}{\partial t} + \left(\frac{\partial \phi}{\partial x} + \Omega \eta \right) \frac{\partial \eta}{\partial x} - \frac{\partial \phi}{\partial y} = 0 \quad \text{at } y = \eta(x, t) \quad (2.8)$$

$$\frac{\partial \phi}{\partial t} + \frac{1}{2} \left\{ \left(\frac{\partial \phi}{\partial x} \right)^2 + \left(\frac{\partial \phi}{\partial y} \right)^2 \right\} + \Omega \eta \frac{\partial \phi}{\partial x} + g \eta - \Omega \psi = \text{const.} \quad \text{at } y = \eta(x, t) \quad (2.9)$$

where Eq. (2.8) expresses the kinematic boundary condition that a fluid particle once on the free surface remains there for all time, whereas Eq. (2.9) is the dynamic boundary condition that the surface pressure is constant.

2.2 Stokes Wave Trains in Uniform Velocity Shear

We now look for wave motion of Stokes type, i.e. periodic waves of permanent form propagating at constant velocity in the x -axis direction. Such waves are steady waves when viewed from a suitable frame of reference Xy where

$$X = x - Ct \quad (2.10)$$

C being an apparent phase velocity of the wave. These steady waves are represented by

$$\phi = -CX + \Phi(X, y) \quad (2.11)$$

$$\eta = \eta(X) \quad (2.12)$$

It is noted that for steady motion the free surface is a streamline corresponding to the constancy of the stream function $\left[\frac{1}{2}\Omega y^2 + \psi \right]_{y=\eta}$. Thus substituting Eq. (2.11) and (2.12) into Eq. (2.4), (2.7) to (2.9), we get

$$\frac{\partial^2 \Phi}{\partial X^2} + \frac{\partial^2 \Phi}{\partial y^2} = 0 \quad (2.13)$$

$$\frac{\partial \Phi}{\partial y} = 0 \quad y \rightarrow -\infty \quad (2.14)$$

$$\left(\frac{\partial \Phi}{\partial X} + \Omega \eta - C \right) \frac{\partial \eta}{\partial X} - \frac{\partial \Phi}{\partial y} = 0 \quad y = \eta(X) \quad (2.15)$$

$$\frac{1}{2} \left\{ \left(\frac{\partial \Phi}{\partial X} + \Omega \eta - C \right)^2 + \left(\frac{\partial \Phi}{\partial y} \right)^2 \right\} + g\eta = \text{const.} \quad y = \eta(X) \quad (2.16)$$

Solutions to Eqs. (2.13) to (2.16) are sought in the form of a power series in a small parameter ϵ characterising the steepness of the waves.

$$\Phi = \epsilon \Phi_1 + \epsilon^2 \Phi_2 + \epsilon^3 \Phi_3 + \dots \quad (2.17)$$

$$\eta = \epsilon \eta_1 + \epsilon^2 \eta_2 + \epsilon^3 \eta_3 + \dots \quad (2.18)$$

$$C = C_0(1 + \epsilon \delta_1 + \epsilon^2 \delta_2 + \dots) \quad (2.19)$$

By use of standard singular perturbation technique for calculating Stokes wave trains, the terms in the series (2.17) - (2.19) can be calculated successively. The results are

$$\Phi_1 = e^{ky} \sin kx X$$

$$\eta_1 = \cos kx X$$

$$\Phi_2 = \frac{1}{4} \bar{\Omega}(\bar{\Omega} + 3) e^{2ky} \sin 2kx X \quad (2.20)$$

$$\eta_2 = -\frac{1}{4}\bar{\Omega}(\bar{\Omega}+2) + \frac{1}{4}(\bar{\Omega}^2+4\bar{\Omega}+2)\cos 2kx$$

and

$$C = C_0 \left[1 + \epsilon^2 \frac{1+2\bar{\Omega} + \frac{5}{4}\bar{\Omega}^2 - \frac{1}{8}\bar{\Omega}^4}{2+\bar{\Omega}} \right] \quad (2.21)$$

where

$$\bar{\Omega} = \frac{\Omega}{\omega} \quad (2.22)$$

k being the wave number, $\omega = kC_0$ and

$$C_0 = \sqrt{\frac{g}{k(1+\bar{\Omega})}} \quad (2.23)$$

§3. Evolution of Stokes Wave Trains in Uniform Velocity Shear

The slow modulation of the Stokes wave train obtained in §2 can be studied by the usual method of multiple scales (Refs 2 & 3) applied to Eq. (2.4), (2.7) - (2.9). In particular, let

$$\eta = \epsilon A(\xi, \tau) e^{i(kx - \omega t)} + \text{complex conjugate} \quad (3.1)$$

together with a compatible expression for ϕ , where

$$\xi = \epsilon(x - c_g t) \quad (3.2)$$

$$\tau = \epsilon^2 t \quad (3.3)$$

c_g being the linear group velocity. Then the evolution of A is governed by the following equation

$$i \frac{\partial A}{\partial \tau} + \mu \frac{\partial^2 A}{\partial \xi^2} = q |A|^2 A \quad (3.4)$$

where

$$\mu = \frac{\omega}{8k^2} \frac{(1+\bar{\Omega})^2}{(1+\bar{\Omega}/2)^3} \quad (3.5)$$

$$q = -\frac{1+2\bar{\Omega}+\frac{5}{4}\bar{\Omega}^2-\frac{1}{8}\bar{\Omega}^4}{2+\bar{\Omega}} \omega k^2 \quad (3.6)$$

The Stokes wave solution of §2 corresponds to the special solution of Eq. (3.4) with

$$A = a_0 e^{-i\frac{1}{2}\bar{\Omega}\tau} \quad (3.7)$$

§4. Stability of Stokes Wave Trains in Uniform Velocity Shear

A standard linear stability analysis (e.g. Ref 4) shows that the stability of the Stokes wave train depends solely on the sign of μq : it is stable when $\mu q > 0$ and unstable when $\mu q < 0$. The maximum growth rate of the side-band, when

normalized by $\frac{1}{2}\omega a_0^2 k^2$, is equal to

$$\frac{1+2\bar{\Omega}+\frac{5}{4}\bar{\Omega}^2-\frac{1}{8}\bar{\Omega}^4}{1+\bar{\Omega}/2} \quad (3.8)$$

This is plotted in Fig 1, which shows that small velocity shear Ω/ω tends to enhance side-band instability, whereas large velocity shear tends to suppress instability.

§5. Comparisons with Experiments

A series of experiments on mechanically generated water waves with wind blowing over them have been conducted in the wind-wave flume of Canada Centre for Inland Waters, Burlington, Ontario. Fig 2 shows the frequency spectra at fetches of 12.0, 24.1 and 34.2 m for wind speeds of 1.4 m/s and 10.5 m/s. It is clear that gentle wind at 1.4 m/s (hence smaller velocity shear generated in the wave field) tends to enhance side-band instability whereas stronger wind at 10.5 m/s (hence larger velocity shear) tends to suppress side-band instability. These, and the similar experimental results of Ref 1, are in qualitative agreement with our theoretical predictions.

Attempts to give a quantitative comparison between experiments and our simplistic theoretical model are, however, met with the difficulty of assigning an appropriate linearized velocity shear to the experimental results. The wind-induced velocity shear is highly nonlinear and the best one can do is estimate lower and upper bounds for the equivalent linear shear. An estimate of the upper bound may be deduced from Kinsman's formula (Ref 5) for the surface shear. This yields a range of Ω/ω from -0.1 to 18.3 for our experiments. An estimate of the lower bound may be based on a linear gradient from the drift velocity of the surface, approximately 3% of the wind speed, to the point of zero velocity in the tank (about 20% of the depth from the surface). This yields a range of Ω/ω from 0.02 to 0.17. Thus, appropriate linear velocity shear may be in the range of 0 to 4.0 in which the theoretical calculations yield first an increase of side-band growth rates and then a decrease. It is encouraging that this is the behavior observed, but quantitatively the prediction and experimental results (Fig 3) differ by a factor of 3. It is clear that a more realistic velocity shear, e.g. an exponential one, will have to be incorporated in the theory before more precise agreement with observations is to be expected.

References

1. Bliven, L.F., Huang, N.E. and Long, S.R., J. Fluid Mechanics, 162, 237, 1986.
2. Hasimoto, H. and Ono, H., J. Phys. Soc. Japan, 33, 805, 1972.
3. Hui, W.H. and Hamilton, J., J. Fluid Mechanics, 93, 117, 1979.
4. Lonquet-Higgins, M.S., Proc. Roy. Soc. Lond., A347, 311, 1976.
5. Kinsman, B., Wind Waves, Prentice Hall, 1965.

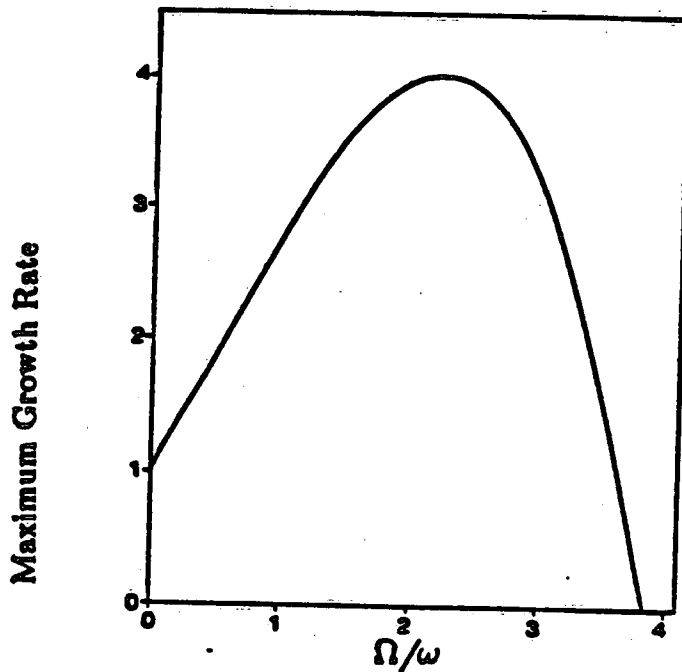


Fig 1. Maximum side-band growth rate vs vorticity.

(a)

(b)

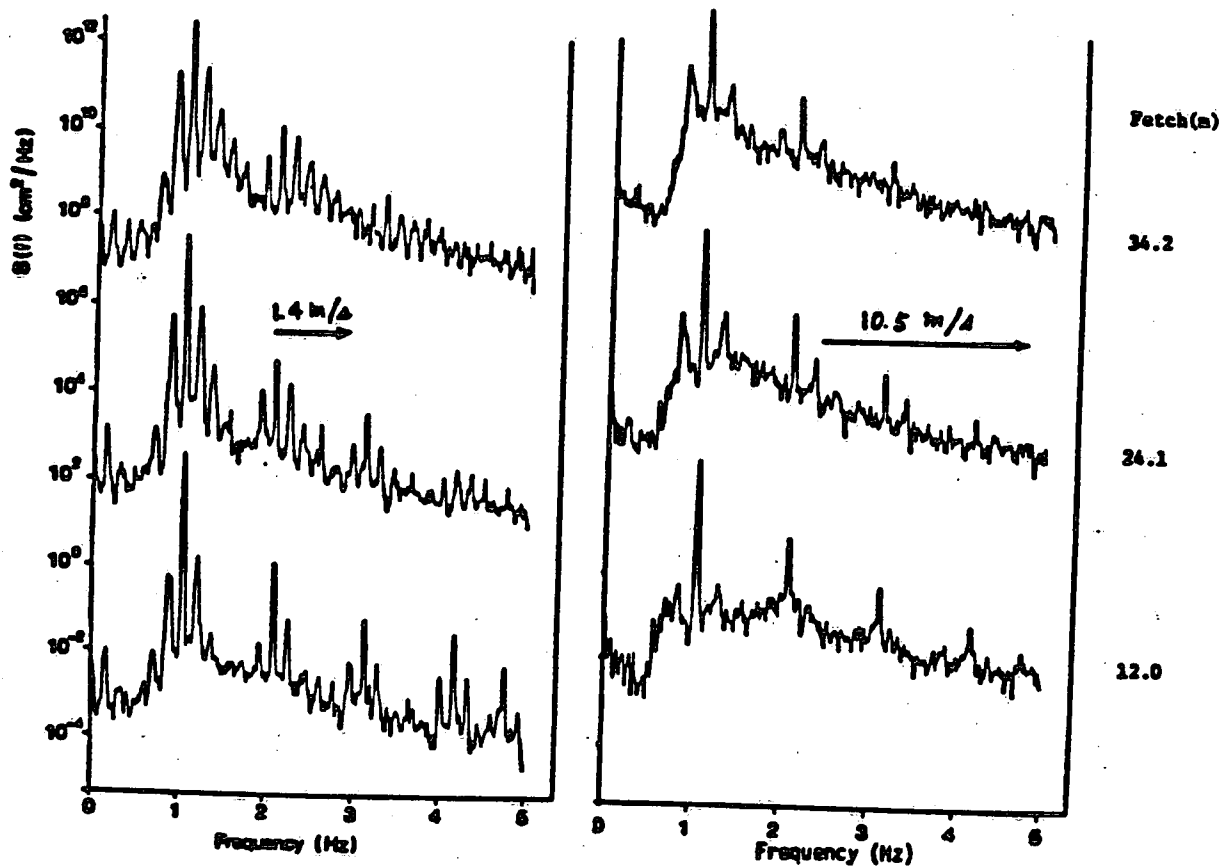


Fig 2. Frequency spectra at fetches of 12.0, 24.1, 34.2 m. The logarithmic ordinate corresponds to the bottom spectrum (at 12.0 m fetch); the others are offset in increments of 5 decades. Resolution bandwidth = 0.0186 Hz, Nyquist frequency = 10 Hz, 32 degrees of freedom.

(a) Low wind speed, 1.4 m/s at 35cm height,

(b) High wind speed, 10.5 m/s.

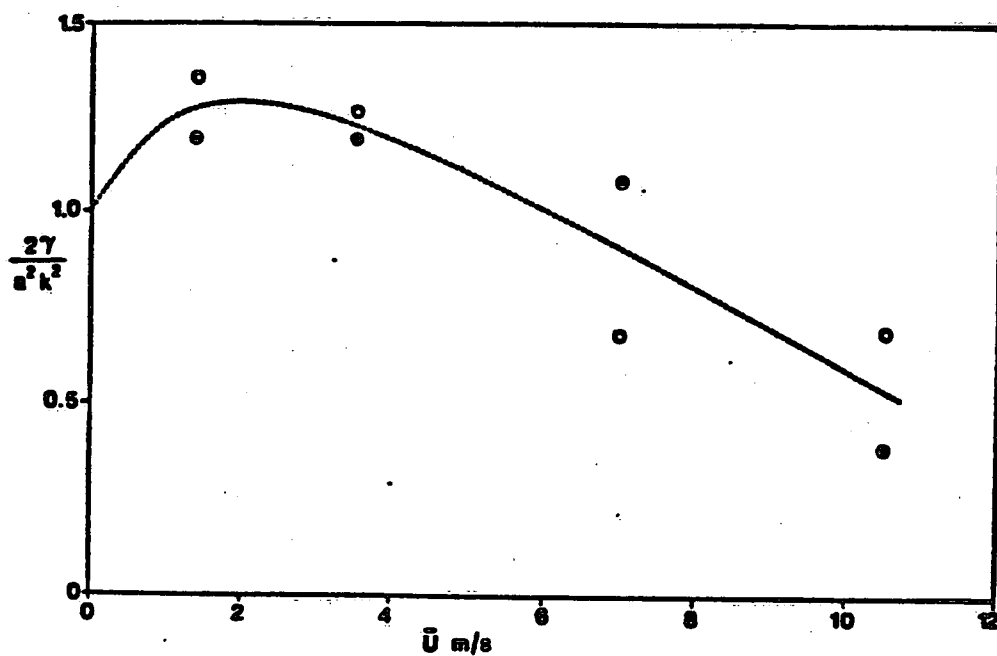


Fig 3. The observed growth rate for the fastest growing side-bands for various wind speeds. The open circles correspond to the low frequency side-band; the closed circles to the high frequency side-band.